International Journal of Mechanical and Materials Engineering (IJMME), Vol. 2 (2007), No. 2, 139--149.

CLASSIFICATION OF DIFFERENT APPROACHES BASED ON MODELLING AND SIMULATION FOR A KINEMATIC ANALYSIS OF PLANAR AND SPATIAL MECHANISM

A. Rastgo, R. Kavlani
Faculty of Mechanical Engineering,Tehran University
North Kargar Ave, Tehran, IRAN
arastgo@ut.ac.ir

ABSTRACT

In finding a complete kinematic analysis of a planer or spatial mechanism; the first step is, asking yourself which approach is ideal. Here we show how the classification of different ways based on modelling and simulation act through particular problems and see if it is always logical to go through the problem without use of any software and also see that simulating a mechanism by software, leads to a fabulous save in time.

Keywords: Planar and Spatial Mechanisms, Graphical Approach, Numerical Methods, Closed-Form Techniques and Stewart Platform.

1 INTRODUCTION

A principal goal of kinematic analysis is to determine the accelerations of all moving parts in assembly. The reason is that dynamic forces are proportional to acceleration and we need to know the dynamic forces in order to calculate the stresses in the components. In order to calculate the accelerations, we must first find the positions of all the links or elements in mechanism for each increment of input motion, and then differentiate the position equations versus time to find velocities, and then differentiate again to obtain the expressions for acceleration.

This can be done by any of several methods. We could use a graphical approach to determine the position, velocity, and acceleration for all 180 positions of interest, or we could derive the general equations of motion for any position, differentiate for velocity and acceleration, and then solve these analytical expressions for our 180 (or more) crank locations. A computer will make this latter task much more palatable [1].

Although graphical method can be used in making a check point in using software; in any case it is not a good idea to use this approach in analysis of a spatial mechanism. So we should use analytical methods. We should say that kinematic motion analysis and design of mechanical systems lead naturally to system of nonlinear algebraic and/or transcendental equations. One of the most frequently occurring problems in kinematics is to find solutions to this system of equations. The solution approaches for such equations can be broadly divided into two classes: numerical (iterative) methods and closed-form (analytical) techniques. Numerical techniques rely heavily on numerical iteration while closed-form techniques are based on analytical expressions and often require massive algebraic manipulations.

Using numerical methods, a kinematics problem is considered solved if a tight upper bound on the number of solutions can be established, and an efficient algorithm for computing all solutions can be implemented. The commonly used iterative methods are variants of either the Newton or conjugate gradient methods. These methods require an initial guess at the solution. If the initial guess is not close enough to a solution, the iterations may converge slowly, converge to an unacceptable solution or may diverge altogether. However, the Newton's method is a valuable tool and is used as the building block for numerical continuation methods. Thus numerical continuation (homotopy) methods have been used in solving kinematic equations of motion for planar as well as spatial mechanisms [2].

Analytical or closed-form solutions to kinematic equations can be obtained using elimination theories based on resultants or Grobner bases [3]. In general, there are two types of eliminates. The first is concerned with the elimination of one variable in two polynomials. The commonly used resultant matrices for such problems are those of Sylvester and Bezout. These resultants are particularly effective in eliminations involving non-homogeneous polynomials.

Here we solve different examples with various methods to compare them with each other. The methods we choose here are tried to the best of their kind. We select Newton method from iterative approaches to solve a four bar 1 DOF mechanism, the method of center of zero velocity from graphical methods to solve a 8-bar mechanism [4,5]. We solve this mechanism also with Grobner-Sylvester hybrid method for closed-form displacement analysis of mechanisms which is selected from closed form solutions to a mechanism [6]. Again we use this method in analysis of a 6 DOF Stewart mechanism which we simulate it in

Simulink MATLAB to show the application of using software in analysis of a mechanism.
We do not discuss all of method's fundamentals, and we concentrate on solving different examples to compare different approaches.

2 Newton-Raphson Solution for the Four bar Linkage

The vector loop equation of the four bar linkage (Fig.1) separated into it's real and imaginary parts provides the set of functions that define the two unknown link angles θ_3 and θ_4.The link lengths a, b, c, d, and the input angle θ_2 are given. So we have:

$$f_1 = a.\cos(\theta_2) + b.\cos(\theta_3) - c.\cos(\theta_4) - d = 0 \quad (1.a)$$

$$f_2 = a.\sin(\theta_2) + b.\sin(\theta_3) - c.\sin(\theta_4) = 0 \quad (1.b)$$

$$B = \begin{bmatrix} a.\cos(\theta_2) + b.\cos(\theta_3) - c.\cos(\theta_4) - d \\ a.\sin(\theta_2) + b.\sin(\theta_3) - c.\sin(\theta_4) \end{bmatrix} \quad (2)$$

The error vector is:

$$X = \begin{bmatrix} \Delta\theta_3 \\ \Delta\theta_4 \end{bmatrix} \quad (3)$$

The partial derivatives are:

$$A = \begin{bmatrix} \frac{\partial f_1}{\partial \theta_3} & \frac{\partial f_1}{\partial \theta_4} \\ \frac{\partial f_2}{\partial \theta_3} & \frac{\partial f_2}{\partial \theta_4} \end{bmatrix} = \begin{bmatrix} -b.\sin(\theta_3) & c.\sin(\theta_4) \\ b.\cos(\theta_3) & -c.\cos(\theta_4) \end{bmatrix} \quad (4)$$

As we know this matrix is known as the Jacobean of the system, and, in addition to its usefulness in this solution method it also tells something about the solvability of the system.

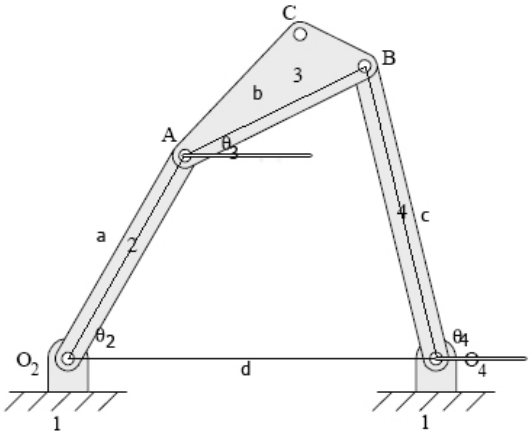

Fig.1. A four bar 1-DOF mechanism.

The system of equations for position, velocity and acceleration (in all of which the Jacobean appears) can only be solved if the value of the determinant of the Jacobean is non zero.
So we'll receive to such equation:

$$\begin{bmatrix} -b.\sin(\theta_3) & c.\sin(\theta_4) \\ b.\cos(\theta_3) & -c.\cos(\theta_4) \end{bmatrix} \begin{bmatrix} \Delta\theta_3 \\ \Delta\theta_4 \end{bmatrix} = -\begin{bmatrix} a.\cos(\theta_2) + b.\cos(\theta_3) - c.\cos(\theta_4) - d \\ a.\sin(\theta_2) + b.\sin(\theta_3) - c.\sin(\theta_4) \end{bmatrix} \quad (5)$$

To solve this matrix equation, guess values will have to be provided for θ_3 and θ_4 and the two equations then solves simultaneously for $\Delta\theta_3$ and $\Delta\theta_4$. For a larger system of equations, a matrix reduction algorithm will need to be used. For simple system in two unknowns, the two equations can be solved by combination and reduction. The test described above which compares the sum of the values of $\Delta\theta_3$ and $\Delta\theta_4$ to a selected tolerance must be applied after each iteration to determine if a root has been found.

3 Grobner-Sylvester Hybrid Method for Closed-Form Displacement Analysis of a 8-Link 1-DOF Mechanism

Consider the 8-link mechanism shown in Fig. 2 with link 5 as the ground. This mechanism does not contain any 4-link loops. The input is provided to link 3 and link 1 is the output link. For this mechanism with three independent loops, namely OABCD, OEFGCD and OEHID, the loop-closure equations are:

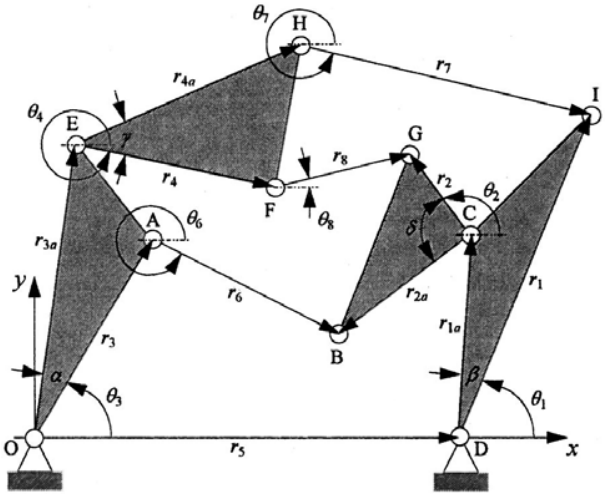

Fig.2. A 8-link 1-DOF mechanism.

$$\mathrm{r}_3.\cos(\theta_3) + r_6.\cos(\theta_6) = r_5 + r_{1a}.\cos(\theta_1 + \beta) + r_{2a}.\cos(\theta_2 + \delta) \quad (6)$$

$$\mathrm{r}_3.\sin(\theta_3) + r_6.\sin(\theta_6) = r_{1a}.\sin(\theta_1 + \beta) + r_{2a}.\sin(\theta_2 + \delta) \quad (7)$$

$$\mathrm{r}_{3a}.\cos(\theta_3 + \alpha) + r_4.\cos(\theta_4) + r_8.\cos(\theta_8) = r_5 + r_{1a}.\cos(\theta_1 + \beta) + r_2.\cos(\theta_2) \quad (8)$$

$$\mathrm{r}_{3a}.\sin(\theta_3 + \alpha) + r_4.\sin(\theta_4) + r_8.\sin(\theta_8) = r_{1a}.\sin(\theta_1 + \beta) + r_2.\sin(\theta_2) \quad (9)$$

$$r_{3a}.\cos(\theta_3 + \alpha) + r_{4a}.\cos(\theta_4 + \gamma) + r_7.\cos(\theta_7) = r_5 + r_1.\cos(\theta_1) \quad (10)$$

$$r_{3a}.\sin(\theta_3 + \alpha) + r_{4a}.\sin(\theta_4 + \gamma) + r_7.\sin(\theta_7) = r_1.\sin(\theta_1) \quad (11)$$

In Eqs. (6) to (11), r_i, θ_3, θ_5, α, β, γ and δ are known and θ_1, θ_2, θ_4, θ_6, θ_7, and θ_8 are unknown. If $\cos(\theta_j)$ and $\sin(\theta_j)$ are treated as algebraic variables with $x_j = \cos(\theta_j)$ and $y_j = \sin(\theta_j)$, then Eqs. (8) to (11) and the trigonometric identity $\sin^2(\theta_j) + \cos^2(\theta_j) = 1$ for j =1, 2, 4, 6, 7, 8, yield a system of 12 algebraic equations in 12 unknowns. Using the dlex term ordering with $x_j < y_j < \ldots$ for j =1, 8, 7, 6, 4, 2 and the method of Grobner bases, the above system of 12 equations leads to the reduced Grobner basis $G=\{g_1,\ldots, g_{29}\}$. Due to space limitations, these polynomials are not reported here. Now consider the numerical data given in Table 1.

The polynomials in G can be viewed as a system of 29 equations in 29 unknowns x_8^3, $x_8^2.y_1$, y_7^2, $x_7.y_7$,

Table.1 Numerical data of the 8-bar mechanism

$y_8.y_7$, $x_7.y_8$, y_8^2, $y_7.x_8$, $x_8.x_7$, $y_8.x_8$, x_8^2, $y_7.y_1$, $y_1.x_7$, $y_1.y_8$, $x_8.y_1$, y_1^2, y_2, x_2, y_4, x_4, y_6, x_6, y_7, x_7, y_8, x_8, y_1 and 1, with coefficients $a_{ij} \in k[x_{ij}]$. The determinant of 29×29 Sylvester's (coefficient) matrix yields the 16th order I/O polynomial in $x_1(=\cos(\theta_1))$:

$$\begin{aligned} F_{I/O} &= x_1^{16} - 2.300807210x_1^{15} \\ &+ 9.154401868x_1^{14} + 0.1203191792x_1^{13} \\ &- 10.46924935x_1^{12} + 31.75664714x_1^{11} \\ &- 11.06912500x_1^{10} - 8.465327682x_1^{9} \\ &+ 50.66174232x_1^{8} - 26.34720696x_1^{7} \\ &- 2.852887181x_1^{6} + 30.78856558x_1^{5} \\ &- 25.56451701x_1^{4} + 3.960569625x_1^{3} \\ &+ 10.2877008x_1^{2} - 7.132207031x_1^{1} \\ &+ 1.232747445 = 0 \end{aligned} \quad (12)$$

Here the entire set of generators (polynomials) in G are needed to set up the Sylvester's matrix because all links fully participate in the mechanism motion. Hence there exists no subset of G that can be used to derive the I/O polynomial since no decoupling in the generators of G is possible. Since all unknown variables y_1, x_j, y_j, for j =2, 4, 6, 7, 8 appear linearly in the monomials column matrix, each of the 11 unknown variables can be expressed linearly in terms of x_j. Hence, this eight-link mechanism has a total of 16 possible assembly configurations (real and complex).

4 Velocity Analysis of a 8-Link Mechanism: Graphical Approach

A schematic drawing of the double butterfly linkage, a 1-DOF 8-link mechanism, is shown in Fig. 3. At first it seems hard to find all of the centers of zero velocity. There are some techniques with which this problem can be solved which you can find them in [7,8,9]. But we choose one that is the most interesting.

We do not discuss in full details which can find them in [10].

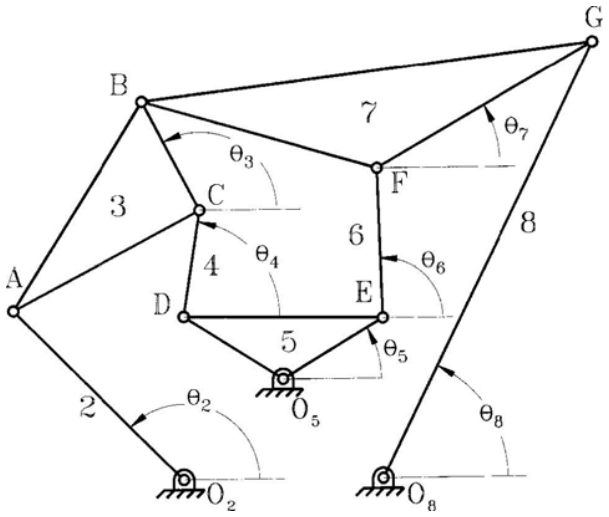

Fig.3. A 8-link 1-DOF mechanism (double butterfly linkage).

We just go through the solution and the method is taken here briefly:

1. Find the point of intersection of link 4 (or link 4 extended) with the line through O_5 that is parallel to link 2. Through this point, draw a line parallel to the line between point B and the point of intersection of links 2 and 4. (See Fig. 4.a)

2. Find the point of intersection of link 6 (or link 6 extended) with the line through O_5 that is parallel to link 8. Through this point, draw a line parallel to the line between point B and the point of intersection of links 6 and 8. (See Fig. 4.b).

3. Denote the point of intersection of the two lines that are drawn in steps 1 and 2 as point Q. (See Fig. 5). Draw a line connecting point Q to the ground pivot O_5 .

4. Draw a line through the coupler point B parallel to the line QO_5 (See Fig. 6). The intersection of this line with link 2 (or link 2 extended) is the instant center I_{13} , and the intersection of this line with link 8 (or link 8 extended) is the instant center I_{17} .

Table.1 Numerical data of the 8-bar mechanism

r_1=13.00	r_2=6.90	r_2=6.90	$r_{4=}$7.00
r_5=15.00	r_6=4.70	r_7=23.50	r_8=6.00
r_{1a}=3.50	r_{2a}=2.50	r_{3a}=10.00	r_{4a}=7.50
$\alpha = \pi / 2$	$\beta = \pi / 2$	$\delta = \pi / 2$	$\gamma = \pi / 2$
$\theta_3 = 21.00$			

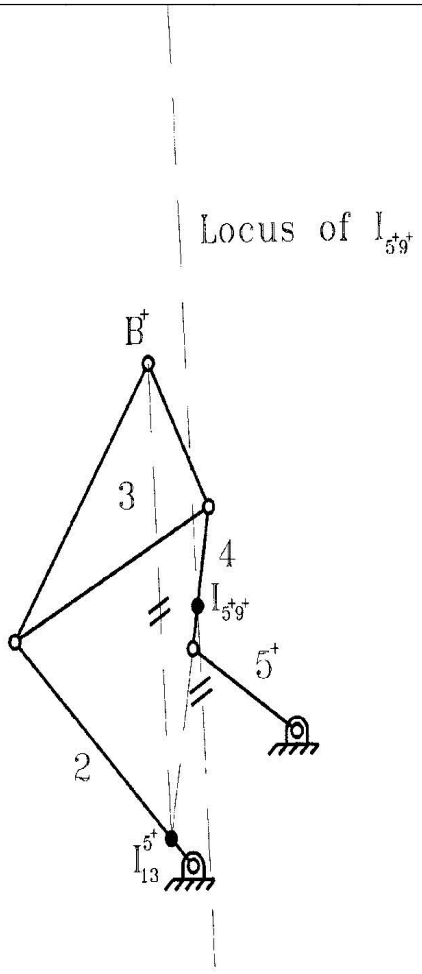

(a)

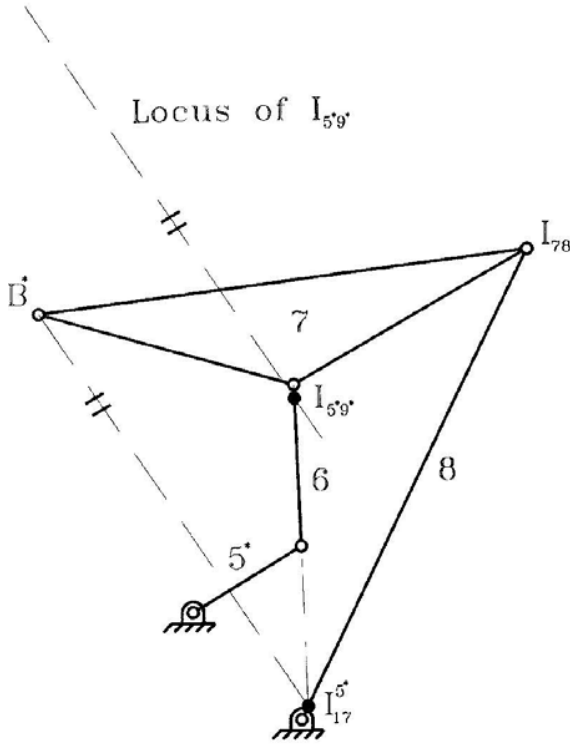

(b)

Fig.4. The lucos of the instant centers (a) $I_{5^+9^+}$ (b) $I_{5^*9^*}$.

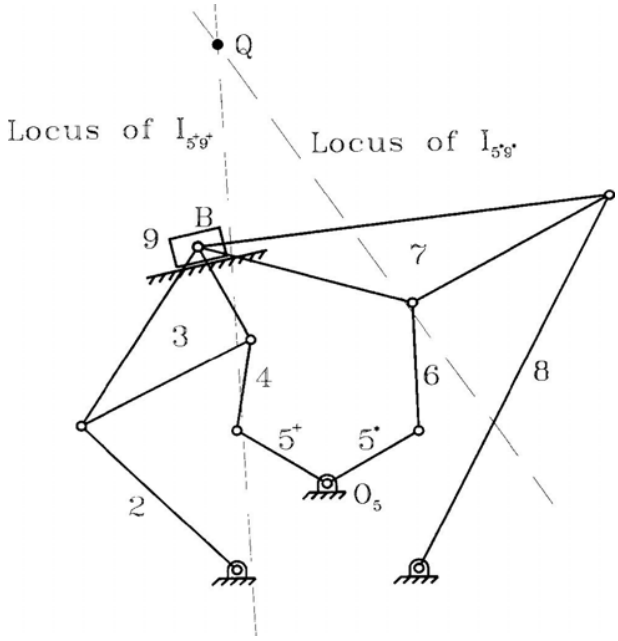

Fig.5. The 8-bar mechanism virtually developed to a ten bar linkage.

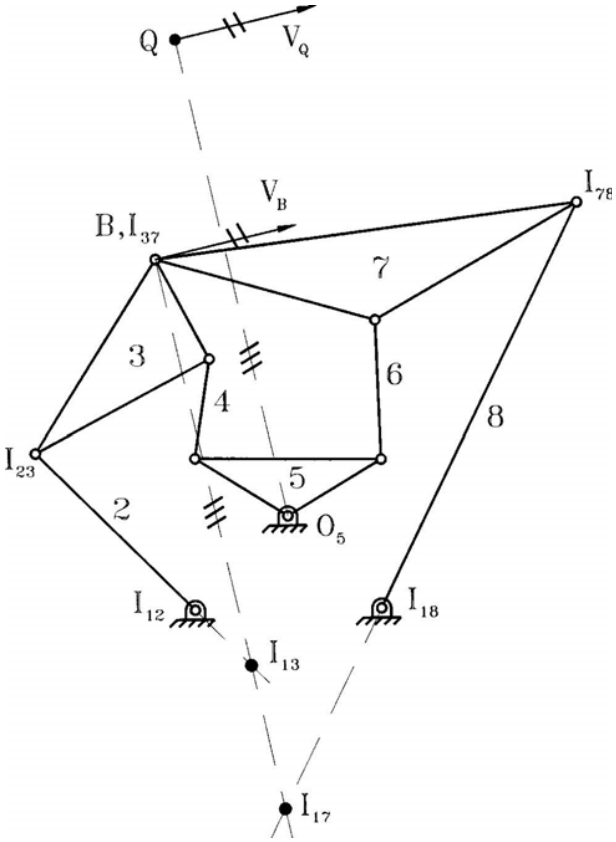

Fig.6. The Instant centers of I_{13} & I_{17}.

And now it is time to go to numerical calculations. Consider again Fig. 3 with the link dimensions tabulated in Table 2. (the link lengths are specified to the nearest 0.01_{cm}). For the chosen position of the input link 2 (i.e., θ_2=135º counterclockwise from the horizontal axis), the position solution is obtained from a vector loop analysis of the linkage and a MATLAB computer program. The results of the angular position of each link are included in Table 2. The linkage was drawn to scale using AutoCAD and the joint angles were specified to the nearest 0.01°. For the specified input position, assume that the angular velocity of the input link 2 is $1_{rad/s}$ clockwise. The angular velocity of link *j* (=3, 4, 5, 6, 7, and 8) can be expressed in terms of the angular velocity of input link 2 and the instant centers as:

$$\omega_j = \frac{I_{12}.I_{2j}}{I_{1j}.I_{2j}}.\omega_2 \qquad (13)$$

Therefore, the angular velocity of the coupler links 3 and 7 can be written, respectively, as:

$$\omega_3 = \frac{I_{12}.I_{23}}{I_{13}.I_{23}}.\omega_2 \quad and \quad \omega_7 = \frac{I_{12}.I_{27}}{I_{17}.I_{27}}.\omega_2 \qquad (14)$$

The location of the secondary instant centers I_{13} and I_{17} are shown on Fig. 6 and the distances between the instant centers are measured on the AutoCAD drawing of the linkage. The location of the remaining secondary instant centers are not shown on the figure, however, the complete set of results are presented in Table 3.

Table.2 Numerical data of the 8-bar mechanism
The link dimensions and angular position of each link

Links	Link Dimensions	Angular Position of each Link
1	O_2O_8=5.00$_{cm}$ O_2O_5=O_5O_8=3.54$_{cm}$	θ_1=0º
2	O_2A=6$_{cm}$	θ_2=135.00º
3	BC=3.05$_{cm}$, AB=6.10$_{cm}$ AC=5.28$_{cm}$	θ_3=117.87º
4	CD=2.68$_{cm}$	θ_4=81.29º
5	O_5D=O_5E=2.93$_{cm}$ DE=5.00$_{cm}$	θ_5=30.76º
6	EF=3.72	θ_6=92.07º
7	BF=FG=6.12$_{cm}$ BG=11.35$_{cm}$	θ_7=29.95º
8	O_8G=12.00$_{cm}$	θ_8=63.96º

Table.3 Location of the instant centers and angular velocity of link j

Link j	$I_{12}I_{2j}$	$I_{1j}I_{2j}$	Angular Velocity of Link j
3	6.00$_{cm}$	8.1114$_{cm}$	0.7397$_{rad/s}$
4	7.6160$_{cm}$	3.9705 $_{cm}$	1.9181 $_{rad/s}$
5	6.0730$_{cm}$	9.6.81 $_{cm}$	0.6320 $_{rad/s}$
6	13.3022$_{cm}$	7.9854 $_{cm}$	1.6658 $_{rad/s}$
7	7.0529	12.9221$_{cm}$	0.5458 $_{rad/s}$
8	22.3882$_{cm}$	27.3884$_{cm}$	0.8174 $_{rad/s}$

Substituting the appropriate values into Eq. (14):

$$\omega_3 = \frac{6.00}{8.1114} \times 1 = 0.7397_{rad/s} \quad clockwise \qquad (15.a)$$

$$\omega_7 = \frac{7.0529}{12.9221} \times 1 = 0.5458_{rad/s} \quad clockwise \qquad (15.b)$$

And as we have Eq. (13):

$$\omega_8 = \frac{I_{12}.I_{28}}{I_{18}.I_{28}}.\omega_2 \qquad (16)$$

Substituting the measured values, see Table 3, and the specified input angular velocity into this equation, the angular velocity of link 8 is:

$$\omega_8 = \frac{22.3882}{27.3884} \times 1 = 0.8174_{rad/s} \quad clockwise \qquad (17)$$

The magnitude of the velocity of the coupler point *B* can be written as:

$$V_B = (I_{13}B)\omega_3 \qquad (18)$$

where the distance $I_{13}B$=11.1817 cm. Substituting this measurement and Eq. (17) into Eq. (18), the magnitude of the velocity of point *B* is:

$$V_B = 8.22411_{cm/s} \qquad (19)$$

The direction of the velocity of point *B* is inclined at 12.20° above the horizontal axis, as shown in Fig. 6. The magnitude of the velocity of the coupler point *B* can also be written as:

$$V_B = V_Q = (I_{15}B)\omega_3 \qquad (20)$$

Therefore, the angular velocity of link 5 can be written as:

$$\omega_5 = \frac{V_B}{I_{15}Q} \qquad (21)$$

Where, from the AutoCAD drawing of the linkage, the distance $I_{15}Q$=13.0872$_{cm}$. Substituting this measurement and Eq. (19*)* into Eq. (21), the angular velocity of link 5 is:

$$\omega_3 = \frac{8.2711}{13.0872} \times 1 = 0.6320_{rad/s} \quad clockwise \qquad (22)$$

The angular velocity of links 4 and 6 can be obtained in a straightforward manner from Eq. (12) and the results

are included in Table 3. The results are in very close agreement with analytical calculations that were performed using Working Model 2D and Microsoft Excel.

5 Forward Displacement Analysis of General Stewart Mechanism

Consider the 6-DOF general Stewart mechanism shown in Fig. 7. The six inputs are provided at the prismatic joints in each leg, which in turn controls the location and orientation of the upper platform. For both moving and fixed platforms, the spherical joints P_i and X_i, $i = 1, \ldots, 6$, are not restricted

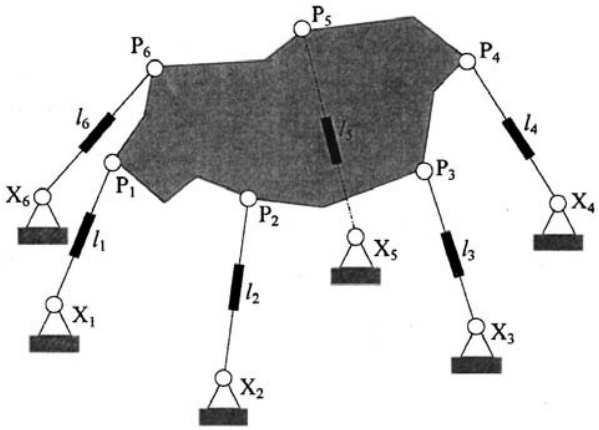

Fig.7. A 6-DOF general Stewart mechanism.

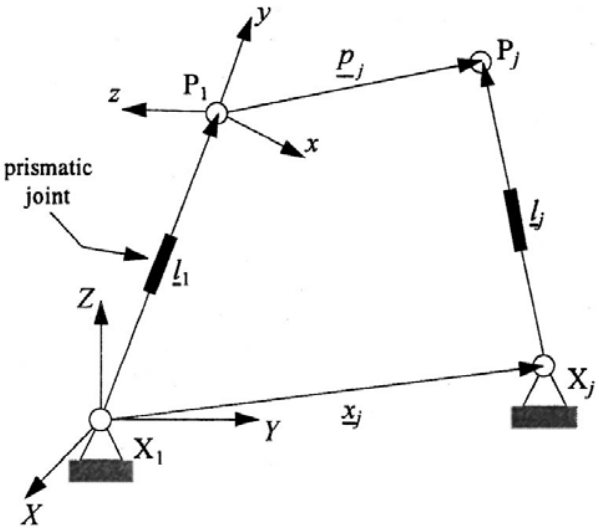

Fig.8. A loop of general Stewart mechanism.

to lie in a plane. The notation and the loop-closure equations are given as follows (see Fig. 8).

Let $\overrightarrow{x_j}$ denote the vector from the origin of the global system to the grounded spherical pair X_j, $\overrightarrow{p_j}$ denote the vector (expressed in moving frame) from the origin of the coordinate frame attached to the platform at P_1 to the spherical pair P_j, $\overrightarrow{l_j}$ denote the vector from the ground spherical pair X_j to moving spherical pair P_j expressed in the base coordinate frame with l_{xj}, l_{yj} and the l_{zj} being the x-, y- and z-components of vector $\overrightarrow{l_j}$, $[R]$ is the 3×3 rotational matrix (of direction cosines) denoting the orientation of the moving frame relative to the base frame, and x_j, l_1, l_j and p_j denote the magnitudes of the vectors $\overrightarrow{x_j}$, $\overrightarrow{l_j}$, $\overrightarrow{l_j}$ and $\overrightarrow{p_j}$, respectively.

Then, the loop-closure equations for the mechanism are:

$$\overrightarrow{l_j} = \overrightarrow{l_1} + [R]\overrightarrow{p_j} - \overrightarrow{x_j}, \quad j = 2,\ldots,6 \tag{23}$$

Equating the magnitudes of the vectors on the left- and right- hand-side of Eq. (23) as:

$$\overrightarrow{l_j}.\overrightarrow{l_j} = (\overrightarrow{l_1} + [R]\overrightarrow{p_j} - \overrightarrow{x_j}).(\overrightarrow{l_1} + [R]\overrightarrow{p_j} - \overrightarrow{x_j}) \tag{24}$$

leads to:

$$\begin{aligned} & l_j^{\,2} = l_1^{\,2} + x_j^2 + p_j^2 \\ & + 2\overrightarrow{l_1}.[R]\overrightarrow{p_j} - 2\overrightarrow{x_j}.[R]\overrightarrow{p_j} - 2\overrightarrow{l_1}.\overrightarrow{x_j} \end{aligned} \tag{25}$$

and after expanding:

$$\begin{aligned} & 2h_1(p_{xj}) + 2h_2(p_{yj}) + 2h_3(p_{zj}) \\ & + p_j^2 + l_1^2 + x_j^2 - l_j^2 \\ & - 2[(p_{xj})r_1 + (p_{yj})r_2 + (p_{zj})r_3]x_{xj} \\ & - 2[(p_{xj})r_4 + (p_{yj})r_5 + (p_{zj})r_6]x_{yj} \\ & - 2[(p_{xj})r_7 + (p_{yj})r_8 + (p_{zj})r_9]x_{zj} \\ & - 2l_{x1}(x_{xj}) - 2l_{y1}(x_{yj}) - 2l_{z1}(x_{zj}) \\ & = 0 \qquad j = 2,\ldots,6 \end{aligned} \tag{26}$$

where

$$\begin{aligned} h_1 &= l_{x1}.r_1 + l_{y1}.r_4 + l_{z1}.r_7 \\ h_2 &= l_{x1}.r_2 + l_{y1}.r_5 + l_{z1}.r_8 \\ h_3 &= l_{x1}.r_1 + l_{y1}.r_6 + l_{z1}.r_9 \end{aligned} \tag{27}$$

and (r_1 ,r_2 ,r_3), (r_4 ,r_5 ,r_6), (r_7 ,r_8 ,r_9) represent the three rows of the rotation matrix [R]. Since [R] is orthogonal, the rows and columns of [R] satisfy the following dot- and cross-product relations

$$\begin{aligned} r_1^2 + r_4^2 + r_7^2 &= 1 \\ r_2^2 + r_5^2 + r_8^2 &= 1 \\ r_3^2 + r_6^2 + r_9^2 &= 1 \\ r_7^2 + r_8^2 + r_9^2 &= 1 \end{aligned} \tag{28}$$

$$\begin{aligned} r_1.r_2 + r_4.r_5 + r_7.r_8 &= 0 \\ r_1.r_3 + r_4.r_6 + r_7.r_9 &= 0 \\ r_2.r_3 + r_5.r_6 + r_8.r_9 &= 0 \end{aligned} \tag{29}$$

$$\begin{aligned} r_7 &= r_2.r_6 - r_3.r_5 \\ r_8 &= r_3.r_4 - r_1.r_6 \\ r_9 &= r_1.r_5 - r_2.r_4 \end{aligned} \tag{30}$$

The constant length condition of vector l_1 is expressed as:

$$l_1^2 = l_{x1}^2 + l_{y1}^2 + l_{z1}^2 \tag{31}$$

The direct kinematics problem can now be stated as follows: for specified leg lengths l_j, for j=1, . . . , 6, determine all possible assembly configurations (real and complex) of the mechanism in terms of the x-, y- and z-components of the reference leg x_1 , y_1 , z_1 and the nine elements r_1 , . . . ,r_9 of the rotational matrix [R].

The system of Eqs. (26) to (31) represents a system of 19 equations in 15 unknown variables, namely r_1 , . . . ,r_9 , x_1 , y_1 , z_1 , h_1 , h_2 and h_3 . Although only 15 equations (Eqs. (26),(27) and (31) and any 6 equations from Eqs. (28)–(30)) are needed to derive the closed-form I/O polynomial for this mechanism, the fact that additional equations are used may actually improve the reduced Grobner basis computational efficiency, provided that the given over constrained system of equations is finitely solvable. In fact, 11 additional relations can be derived from the dot- and cross products of the orthogonal vectors of the rotational matrix [R] that can be adjoined to Eqs. (26)–(31) to derive the same reduced Grobner basis. It should be emphasized that the reduced Grobner basis and the number of generators used to setup the Sylvester's matrix is independent of the initial number equations used to derive the reduced Grobner basis provided that the initial system of equations is finitely solvable.

Using the dlex term ordering with $r_5 <_T r_4 <_T r_2 <_T r_9 <_T r_8 <_T r_7 <_T r_6 <_T r_3 <_T r_1 <_T l_{z1} <_T l_{y1} <_T l_{x1} <_T h_3 <_T h_2 <_T h_1$, yields a reduced Grobner basis G with 68 polynomials.

For the numerical data given below, the 68 polynomials in G are not reported herein due to space limitations.

Suppressing the unknown r_5, G can be viewed as a linear system of 68 equations in 68 unknown monomials r_2^3, $l_{z1}.r_4^2$, $r_1.r_4^2$, $r_4^2.r_3$, $r_4^2.r_6$, $r_7.r_4^2$, $r_9.r_4^2$, r_4^3, l_{Z1}^2, $r_1.l_{z1}$, r_1^2, $r_3.l_{z1}$,$r_1.r_3$, r_3^2, $l_{z1}.r_6$, $r_1.r_6$, $r_3.r_6$, r_6^2, $l_{z1}.r_7$, $r_1.r_7$, $r_3.r_7$, $r_7.r_6$, r_7^2, $l_{z1}.r_8$, $r_1.r_8$, $r_3.r_8$, $r_8.r_6$, $r_7.r_8$, r_8^2, $l_{z1}.r_9$, $r_1.r_9$, $r_3.r_9$, $r_9.r_6$, $r_7.r_9$, $r_8.r_9$, r_9^2, $r_2.l_{z1}$, $r_1.r_2$, $r_2.r_3$, $r_2.r_6$, $r_2.r_7$, $r_2.r_8$, $r_2.r_9$, r_2^2, $l_{z1}.r_4$, $r_1.r_4$, $r_4.r_3$, $r_4.r_6$, $r_7.r_4$, $r_8.r_4$, $r_9.r_4$, $r_2.r_4$, r_4^2, h_1, h_2 , h_3, l_{x1}, l_{y1}, l_{z1}, r_1, r_3, r_6, r_7, r_8, r_9, r_2, r_4 and 1, with the polynomial coefficients expressed in terms of r_5.

Table.4 Numerical data for Stewart mechanism

p_{x1}=0	p_{y1}=0	p_{z1}=0
p_{x2}=2	p_{y2}=3	p_{z2}=3
p_{x3}=3	p_{y3}=5	p_{z3}=0
p_{x4}=1	p_{y4}=0	p_{z4}=4
p_{x5}=4	p_{y5}=2	p_{z5}=1
p_{x6}=2	p_{y6}=1	p_{z6}=3
x_{x1}=0	x_{y1}=0	x_{z1}=0
x_{x2}=2	x_{y2}=3	x_{z2}=0
x_{x3}=3	x_{y3}=4	x_{z3}=4
x_{x4}=5	x_{y4}=1	x_{z4}=2
x_{x5}=0	x_{y5}=2	x_{z5}=3
x_{x6}=4	x_{y6}=0	x_{z6}=5
l_1=12	l_2=12	l_3=10
l_4=14	l_5=12	l_6=10

$$\begin{bmatrix} g_1 \\ \vdots \\ \\ \\ g_{68} \end{bmatrix} = \begin{bmatrix} 68 \times 68 \\ a_{ij} \in k[r_5] \end{bmatrix} \begin{bmatrix} r_2^3 \\ l_{z1}.r_2^4 \\ \vdots \\ 1 \end{bmatrix} \tag{32}$$

Since G={g_1, . . . , g_{68}}=0, Eq. (32) reduces to SX=0 where S is the 68×68 Sylvester's (or coefficient) matrix and X is the 6831 column matrix of the unknown variables (the 68 monomials).

The vanishing of the Sylvester's matrix determinant, i.e., $|S| = 0$, yields the following univariate resultant:

$$
\begin{aligned}
F_{I/O} &= r_5^{40} - 40.34068436 r_5^{39} + 2613.674295 r_5^{38} \\
&+ 48741.59612 r_5^{37} - 428723.4299 r_5^{36} \\
&- 4274132.197 r_5^{35} - 83540302.79 r_5^{34} \\
&- 1100933043 r_5^{33} + 0.1759214513\text{e}11 r_5^{32} \\
&+ 0.1965350860\text{e}12 r_5^{31} + 0.1048048526\text{e}13 r_5^{30} \\
&- 0.2345420202\text{e}14 r_5^{29} + 0.1519869349\text{e}15 r_5^{28} \\
&- 0.2532142007\text{e}16 r_5^{27} + 0.5763041011\text{e}16 r_5^{26} \\
&- 0.1262508992\text{e}18 r_5^{25} + 0.1708093186\text{e}19 r_5^{24} \\
&- 0.1280226550\text{e}20 r_5^{23} + 0.1277021571\text{e}21 r_5^{22} \\
&- 0.1438435067\text{e}21 r_5^{21} + 0.2959635899\text{e}22 r_5^{20} \\
&- 0.5268108151\text{e}23 r_5^{19} + 0.7036209479\text{e}23 r_5^{18} \\
&- 0.4607232515\text{e}24 r_5^{17} + 0.9532463122\text{e}25 r_5^{16} \\
&- 0.1808866634\text{e}26 r_5^{15} + 0.2100680317\text{e}27 r_5^{14} \\
&- 0.2058612826\text{e}28 r_5^{13} + 0.6893379360\text{e}28 r_5^{12} \\
&- 0.3848331827\text{e}29 r_5^{11} + 0.1749687727\text{e}30 r_5^{10} \\
&- 0.3684514761\text{e}30 r_5^{9} + 0.1092764420\text{e}31 r_5^{8} \\
&- 0.2122101006\text{e}31 r_5^{7} + 0.1577335438\text{e}31 r_5^{6} \\
&+ 0.5167452234\text{e}31 r_5^{5} + 0.4545748611\text{e}31 r_5^{4} \\
&- 0.9804725966\text{e}31 r_5^{3} + 0.9522001983\text{e}31 r_5^{2} \\
&- 0.1610650914\text{e}32 r_5 + 0.9994869958\text{e}31 \\
&= 0
\end{aligned}
\tag{33}
$$

Here $F_{I/O}$ is the 40th degree I/O polynomial for the forward kinematics problem of the general Stewart mechanism and it is devoid of any extraneous factors.

Two items are worth mentioning at this point. First, it is not necessary that the smallest variable in the dlex term order should be hidden to set up the Sylvester's matrix even though it is the case with the example above where r_5 is suppressed. Second, it may be noted that the forty solutions could also have been obtained by solving the generalized eigenvalue problem Eq. (32) instead of expanding the determinant of the Sylvester's matrix. The reason for expanding the determinant of S to derive the univariate I/O polynomial is that this polynomial contains a wealth of other information about Stewart's mechanism such as its singular and unstable configurations which can be determined by analyzing discriminants of Eq. (33).

Hence, the Stewart mechanism has 40 possible solutions (real and complex) since the I/O polynomial in Eq. (33) is a 40th order polynomial and the remaining unknown variables are linear and expressed explicitly in r_5. It should be noted that since [R] is a direction cosine matrix, the elements (r_i) of this matrix must satisfy the additional constraint $|r_i| \le 1$. Otherwise, the solution is considered to be complex since $\cos^{-1}(r_i>1)$ or $\sin^{-1}(r_i>1)$ leads to complex values.

6 Analysis of a Stewart Platform Using Simulink

Now again consider the Stewart mechanism. We saw in spite of using one of the best methods of analytical algorithms, it'll take us so much time just to perform position analysis of that Stewart mechanism.

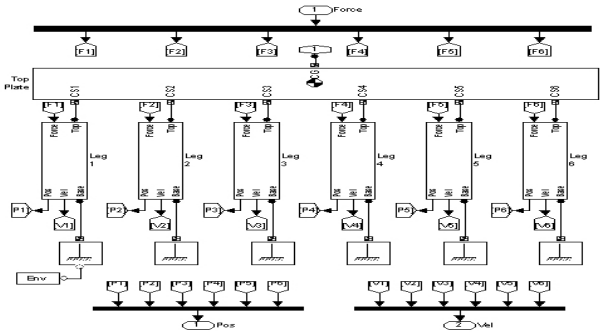

Fig.9. Stewart mechanism modeled in Simulink.

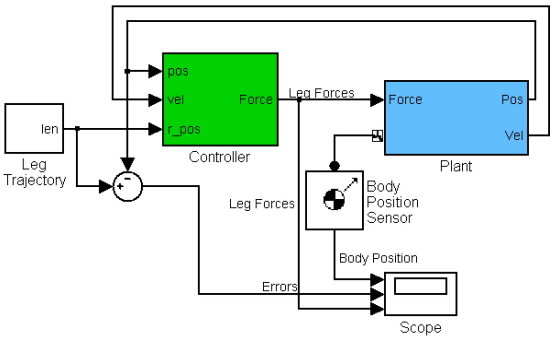

Fig.10. System modeled in Simulink MATLAB.

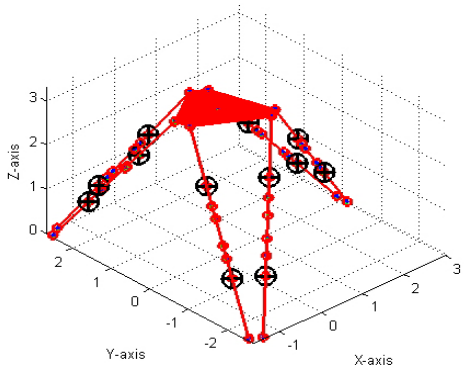

Fig.11. A schematic preview of the mechanism.

So we again go through that mechanism. This time we simulate the mechanism in Simulink MATLAB. (See Fig. 9).

And we put it as a control unit (subsystem) of the control system (Fig. 10). A schematic view of the model is shown in (Fig. 11).
This model can be simulated with any input data and running the model every time leads to results which are needed. For example the curves of displacement,

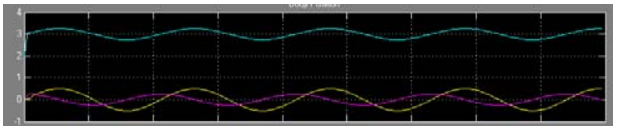

Fig.12. Positin of the center of gravity of the platform vs time.

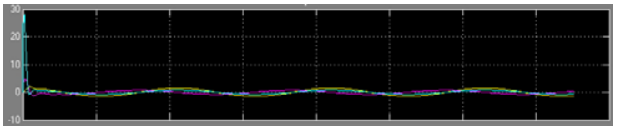

Fig.13. Velocity of the center of gravity of the platform vs time

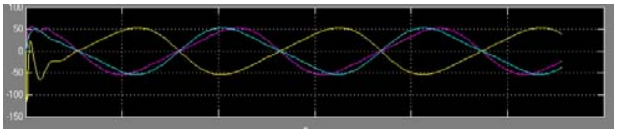

Fig.14. Angular velocity of the center of gravity of the platform vs time.

Fig.15. Angular velocity of the center of gravity of the platform vs time.

velocity, angular velocity, and acceleration of the platform's CG vs time is shown in Figs. 12 to 15.

In any case receiving to such answers is very difficult in practice. See [11,12] for analysis of such mechanisms.

7 CONCLUSIONS

Different approaches were mentioned through various kinds of mechanisms. We saw that iterative methods can be or sometime not useful in depending on the first guess at the solution. So the iterations may diverge, or converge to undesired solutions. It also does not give us a brief aspect of the solution until it reaches to final answer. So other solutions like graphical methods are applicable. The example we selected to solve by this method showed us that scaling a 2D mechanism on the paper leads to a solution to the position analysis. In spite of that we saw that in getting face to face to a velocity analysis problem, graphical methods do not lead us to a straightforward approach. For example the double butterfly linkage we have analyzed here couldn't be solved without use of such tricks mentioned in this text. However the graphical methods in any case are the most tricky; but by that we can not go through a 3D problem without modelling it with special 3D softwares if possible. Thus closed-form solutions may be the most straightforward way to analyze a mechanism. And it also differs from graphical methods in a way that one time you go through it for a set of input data for a mechanism you'll be needless to repeat it for different one. But it still has one disadvantages and that's the large amount of calculations you are involved with using this method; as you saw using one of the best methods of that sort just in position analysis of the Stewart platform mechanism needs a lot of time. And by that method the desired tolerance of the answers can not be gained like that in iterative methods. That's why using softwares is such a suitable approach. We showed that by a software any proposed information is achievable even in analysis of a complicated mechanism like Stewart platform. But something we should never forget is that the methods we mentioned above (analytical and graphical) are always needed in checking the results gained from software. The reason is that an engineer does always consider whether the answers which are resulted from a software are coordinated with data that seems logical due to his or her personal experiments. If such experimental data do not exist as for engineers who are not so experienced; making some checkpoints are unavoidable.

REFERENCES:

[1]G. Erdman, , G. N. Sandor, and S. Kota, *Mechanism Design*, Volume 1, Fourth Edition, Prentice-Hall Inc., Upper Saddle River, New Jersey, 2001.

[2]R. Norton, *Design of Machinery*, 3rd edition, Mc Graw Hill, 2004.

[3]D. Kapur, Y. Cai, *An Algorithm for Computing a Grobner Basis of a Polynomial Ideal Over a Ring with Zero Divisors*, 2003.

[4]D.E Foster, G.D Pennock, *Graphical Methods to Locate the Secondary Instant Centers of Single-Degree-of-Freedom Indeterminate Linkages*, Journal of Mechanical Design, ASME, Vol. 127, 2005.

[5]E.C. Kinzel, *Path Curvature of the Single Flier Eight-Bar Linkage*, 2003.

[6]A.K Dhingra, A.N Almadi,D Kohil, *A Grobner-Sylvester Hybrid Method for Closed-Form Displacement Analysis of Mechanisms*, Journal of Mechanical Design, ASME, Vol. 122, DECEMBER 2000.

[7]Dijksman, E. A., *Why Joint-Joining is Applied on Complex Linkages*, Proceedings of the Second IFToMM International Symposium on Linkages and Computer Aided Design Methods, Vol. II, paper 17, pp. 185–212, SYROM '77, Bucharest, Romania, June 16–21, 1977.
[8]N. Rosenauer, and A. H. Willis, *Kinematics of Mechanisms*, Associated General Publications Pty. Ltd., Sydney, Australia, 1953.
[9]Yan, H-S., and Hsu, M-H., *An Analytical Method for Locating Velocity Instantaneous Centers*, Proceedings of the 22nd Biennial ASME Mechanisms Conference, DE-Vol. 47, Flexible Mechanisms, Dynamics, and Analysis, pp. 353–359, Scottsdale, Arizona, September 13–16, 1992.
[10]D.E Foster, G.D Pennock, *Graphical Methods to Locate the Secondary Instant Centers of Single-Degree-of-Freedom Indeterminate Linkages*, Journal of Mechanical Design, ASME, Vol. 127, 2005.
[11]H. Zohour, H. Pendar, M. Vakil, *Inverse and Forward Kinematics and Singularity Analysis of a Spherically Actuated Platform Manipulator with 3 SPU Legs*, MSc. thesis, Sharif University, Tehran, Iran, 2003.
[12]H. Tavakolinia, K. Sugimuto, H. Zohour, *A Computational Alghorithm with High Generality for Simulation of Parallel Mechanisms*, ASME Transactions, Jurnal of Mechanical Design,Paper No: MD-05-1190, January 2006.